105 (2026) 106950

Contents lists available at ScienceDirect

Poultry Science

journal homepage: www.elsevier.com/locate/psj

Full-Length Article

Single-cell transcriptomic insights into lipoprotein transport in yolk sac membrane endodermal epithelial cells of chicken embryos

Jie-Ci Wu [a], Zhao-Qi Hu [c], Yuan-Yu Lin [a], Harry J. Mersmann [a], Shih-Torng Ding [a,b,*]

[a] Department of Animal Science and Technology, National Taiwan University, Taipei, Taiwan
[b] Institute of Biotechnology, National Taiwan University, Taipei, Taiwan
[c] Institute of Biotechnology and Graduate Institute of Biomedical Electronics and Bioinformatics, National Taiwan University, Taipei, Taiwan

ARTICLE INFO

Keywords:
Chicken embryo
High-density lipoprotein
Lipoprotein transport
Single-cell RNA sequencing
Yolk sac membrane

ABSTRACT

Efficient lipid mobilization from yolk is critical for avian embryonic development, yet the cellular mechanisms governing lipoprotein transport in yolk sac membrane endodermal epithelial cells remain poorly characterized. Single-cell RNA sequencing was performed on 9,037 embryonic day 4 and 6,884 embryonic day 7 chicken yolk sac membrane cells to investigate lipoprotein biosynthesis pathways. Analysis identified 17 transcriptionally distinct clusters, including 3 endodermal epithelial cell subtypes. Cluster 2, characterized by high expression of epithelial markers (CDH1, EPCAM) and HDL biosynthesis genes (APOA1, ABCA1, LCAT), emerged as the primary site of HDL assembly. Apolipoprotein A1 ranked third in expression whereas apolipoprotein B ranked only 63rd, indicating a prominent HDL-biogenesis program in EECs. Gene ontology enrichment revealed upregulation of cholesterol metabolism and lipoprotein particle receptor binding pathways from embryonic day 4 to 7. Temporal expression analysis demonstrated progressive increases in HDL-related genes (APOA1, ABCA1, LCAT, SOAT1) throughout incubation, peaking at embryonic day 20, while VLDL-related genes (APOB, MTTP, SAR1B) showed sustained upregulation. Plasma analysis at embryonic day 19 confirmed HDL concentration (194.78 ± 30.13 mg/mL, mean ± SEM) significantly exceeded VLDL concentration (65.43 ± 13.82 mg/mL; $P < 0.01$), representing approximately 75% of measured lipoproteins. These findings reveal that HDL, rather than VLDL alone, plays a substantial role in lipid redistribution during late chicken embryogenesis, with HDL serving as the primary carrier of cholesteryl esters and phospholipids while VLDL remains the dominant triacylglycerol transporter, highlighting complementary lipoprotein functions and species-specific metabolic adaptations critical for embryonic development.

Introduction

Hatchability strongly influences poultry production efficiency, yet embryonic mortality remains a major constraint, particularly during late incubation when nutrient demands peak (Amer, 1962; Peñuela and Hernandez, 2018). Lipids, as the primary energy source and structural substrates, are critical for supporting rapid embryonic growth. Yadgary et al. (2013) reported that yolk lipid content declines by nearly 50% between embryonic day 11 (E11) and day 21 (E21), underscoring the importance of lipid mobilization during this stage. Inefficient lipid utilization may therefore contribute to compromised embryonic viability and reduced hatchability.

Yolk sac membrane (YSM) proteins involved in nutrient uptake and very low-density lipoprotein (VLDL) synthesis are highly expressed in endodermal epithelial cells (EECs) (Bauer et al., 2013; Yadgary and Wong, 2014). Lipoprotein receptor LR8 mediates recognition of apoB-containing VLDL (Hermann et al., 2000), while dynamin-dependent endocytosis regulates VLDL uptake (Tung et al., 2021). Following absorption, VLDL particles are digested and re-esterified before being repackaged and exported to the circulation (Shand et al., 1993). Cholesterol esterification, catalyzed by sterol O-acyltransferase (SOAT/ACAT) and regulated by AMP-dependent pathways, is essential for lipoprotein assembly (Ding and Lilburn, 2002; Wang et al., 2017). Eresheim et al. (2014) reported that EECs can express microsomal triglyceride transfer protein (MTTP), involving in syntheses of new lipoproteins.

Although the significance of lipid metabolism for embryonic development is well established, the molecular mechanisms governing

* Corresponding author.
E-mail address: sding@ntu.edu.tw (S.-T. Ding).

https://doi.org/10.1016/j.psj.2026.106950
Received 25 December 2025; Accepted 16 April 2026
Available online 17 April 2026
0032-5791/© 2026 The Authors. Published by Elsevier Inc. on behalf of Poultry Science Association Inc. This is an open access article under the CC BY-NC-ND license (http://creativecommons.org/licenses/by-nc-nd/4.0/).

lipoprotein formation and transport remain poorly understood due to the cellular complexity of the YSM. Conventional analyses cannot resolve cell-specific transcriptional programs. Traditional approaches to studying YSM biology rely on bulk tissue analyses of manually dissected membrane layers. However, even careful dissection of the YSM inevitably yields preparations containing multiple cell types, including endodermal epithelial cells, mesenchymal cells, vascular endothelial cells, and hematopoietic progenitors, thereby obscuring cell-type-specific transcriptional programs. Single-cell RNA sequencing (scRNA-seq) provides a powerful strategy to overcome this limitation, by resolving transcriptional profiles at the individual cell level within these complex tissue preparations. Understanding the temporal dynamics of lipoprotein-related gene expression during embryogenesis is essential, as the metabolic demands of the developing embryo shift progressively from reliance on yolk-derived nutrients to endogenous lipid synthesis. Characterizing when specific lipoprotein biosynthesis programs are activated in EECs can reveal how the YSM adapts its transport machinery to meet evolving embryonic requirements. We selected E4 and E7 as time points for scRNA-seq analysis because E4 represents the onset of endodermal epithelial differentiation and initial expression of nutrient transport competence in the YSM (Bauer et al., 2013), while E7 marks a stage at which EECs have acquired functional lipid metabolic capacity. These early time points capture the establishment of lipoprotein biosynthesis programs that underpin the extensive lipid mobilization occurring during later embryogenesis. We hypothesized that single-cell transcriptomic profiling would reveal the principal lipoprotein biosynthesis pathways in EECs and clarify the temporal dynamics of lipoprotein gene expression during embryogenesis, particularly the relative contributions of HDL and VLDL pathways. In this study, scRNA-seq was applied to investigate lipoprotein-related pathways in chicken YSM EECs, aiming to elucidate the transcriptional basis of lipid transport and utilization during chicken embryogenesis.

Materials and methods

Animals and fertilized eggs

All experimental procedures were approved by the Institutional Animal Care and Use Committee of National Taiwan University (Approval No: NTU-112-EL-00195). In this study, fertilized eggs from Lohmann ultra-lite laying hens were used to study the development of YSM during chicken embryonic development. Fertilized eggs were obtained from a reputable commercial farm in Taiwan and incubated at 37°C with 60% relative humidity in a incubator (Hoong sheng incubatory co. LTD, Changhua, Taiwan) with a capacity of 1000 eggs. A total of 84 fertilized eggs were used in this study. Eggs were randomly assigned to incubation groups for each experimental time point. As eggs were sourced from a commercial flock, individual hen identification was not possible; therefore, each egg was treated as an independent biological replicate.

Primary endodermal epithelial cell culture and single cell RNA sequencing (scRNA-seq)

Four biological replicates (eggs from different hens) were used for each time point. Eggs from embryonic day 4 (E4) and E7 were collected. For E4 and E7, eggs were washed with phosphate buffered saline (PBS), and the innermost layers of the YSM, including the endodermal epithelium and associated mesenchymal tissue, were gently peeled from the yolk surface, cut into pieces, and digested in 3 mL type IV collagenase (200 U/mL) at 37°C for 15 minutes to isolate the cells. The cells were then washed with DMEM (Tseng Hsiang Life Science LTD., New Taipei, Taiwan), resuspended in DMEM supplemented with 10% new born calf serum (16010-142, Gibco, USA) and 1% antibiotic (Pen-Strep Ampho. Solution, Sartorius AG, Göttingen, Germany), and evenly cultured in 12-well plates (4×10^6 cells/well) at 37°C with 5% CO_2 for 24 hours. The 24-hour culture step allowed cells to recover from enzymatic digestion and facilitated the removal of non-viable cells and debris, thereby enriching for viable cells suitable for high-quality scRNA-seq library preparation.

Library generation and sequencing

The scRNA-seq libraries were prepared by the Animal Resource Center and the Consortium of Integrative Biomedical Science Key Technology at National Taiwan University using the BD Rhapsody Express Single-Cell Analysis System and BD Rhapsody™ WTA Amplification Kit per the manufacturer's protocol. Briefly, cells were dissociated with 0.5% Trypsin-EDTA (Thermo Fisher Scientific, Waltham, MA, USA), counted using a Countess 3 Automated Cell Counter (Thermo Fisher Scientific, Waltham, MA, USA), and loaded onto the BD Rhapsody cartridge. cDNA synthesis was performed using the Express System cDNA Synthesis Kit (BD Biosciences, Franklin Lakes, NJ, USA). Two rounds of random primer extension were conducted to generate RPE products, which were purified with AMPure XP beads (Beckman Coulter, Brea, CA, USA) to remove primer dimers. The RPE products were then amplified by PCR using PCR MasterMix and WTA Primer for 11–13 cycles (optimized according to cell number), followed by AMPure XP purification. Illumina sequencing adapters and indices were added during Index PCR (8–9 cycles). Final libraries were subjected to double-sided size selection with AMPure XP beads to obtain fragments of 250–1,000 bp. Library quality and quantity were assessed using a Qubit 4.0 Fluorometer (Thermo Fisher Scientific, Waltham, MA, USA) and an Agilent 4200 TapeStation System (Agilent Technologies, Santa Clara, CA, USA). Sequencing was performed on an Illumina NovaSeq X Series platform (Illumina, San Diego, CA, USA) with paired-end 150 bp (PE150) configuration, targeting approximately 50,000 reads per cell.

Genome alignment and quality control

Quality control and downstream analysis were conducted using R (v4.2.0) and the Seurat package (v4.3.0). Raw sequencing reads were aligned to the white leghorn layer genome (NCBI RefSeq: GCF_016700215.2) through read mapping. Stage-specific QC thresholds were applied due to differences in gene detection distributions between developmental stages. For E4, cells with 2,500–6,500 nFeature_RNA and 2,000–22,000 nCount_RNA were retained, yielding 9,037 high-quality cells from an initial ~12,000 cells. For E7, cells with 1,500–6,500 nFeature_RNA and 2,000–22,000 nCount_RNA were retained, yielding 6,884 high-quality cells from an initial ~10,000 cells. The lower minimum nFeature_RNA threshold for E7 was used because a large proportion of E7 cells exhibited nFeature_RNA $<$ 2,000; applying the E4 threshold would have excluded nearly 30% of otherwise high-quality cells. Detailed QC distributions are provided in Supplementary Fig. S1 and Supplementary Table 1-4.

Data normalization and variable gene selection

The 2,000 most highly variable genes (HVGs) were identified using the "FindVariableFeatures" function in Seurat with "Variance Stabilizing Transformation (VST)" to capture genes with significant expression variability across cells. To address differences in sequencing depth, cell transcriptomes were normalized using the "NormalizeData" function with "Log-normalization".

PCA, UMAP, and cell cluster characterization

The selected highly variable feature genes underwent principal component analysis (PCA), with the top 20 principal components used for Uniform Manifold Approximation and Projection (UMAP) to project data into a two-dimensional plane, identifying 17 cell clusters (Clusters 0–16). Heatmaps then characterized these clusters, selecting the top 10

or 20 differentially expressed genes (expressed in ≥25% of cells, Log2 fold change > 0.25, upregulated) per cluster (Supplementary Fig. S2).

GO and KEGG enrichment analyses

To explore metabolic pathways in specific cell clusters, analysis was performed using Python (v3.9.19), gseapy (v1.1.4), pandas (v2.2.2), and matplotlib (v3.8.4) with "KEGG_2021_Human" and "GO_Molecular_Function_2023″ databases. The "enrichr" function assessed significance by FDR-corrected P-values, visualized as Log10 (1/FDR) color mapping.

YSM sample preparation

YSM samples were collected from embryonic days 4, 8, 12, 16, and 20 (E4, E8, E12, E16, E20) as well as 3 days post-hatch (D3). The YSM was washed with PBS to remove the blood and lipid contaminants. Total RNA was extracted from YSM using GENzol^{TM} Reagent (Geneaid, New Taipei City, Taiwan), and quantified with NanoDrop^{TW} One/One^{c} (Thermo Fisher Scientific, Waltham, MA, USA). The RNA was treated with TURBO DNA-free^{TM} kit (Thermo Fisher Scientific, Waltham, MA, USA) to eliminate DNA contamination, then reverse transcribed into cDNA using High Capacity cDNA Reverse Transcription Kit (Thermo-Fisher Scientific).

Real-time quantitative PCR (qPCR) analysis

The expression of HDL-related and VLDL-related genes was evaluated using the SensiFAST^{TM} SYBR No-ROX Kits (Meridian Bioscience Inc., Cincinnati, Ohio, USA) and analyzed with CFX384 Touch Real-Time PCR Detection System (Bio-Rad Laboratories, Hercules, California, USA). The qPCR program was configured as follows: an initial polymerase denaturation step at 95°C for 2 minutes, followed by 40 cycles of denaturation at 95°C for 5 seconds, annealing at 60°C for 10 seconds, and elongation at 72°C for 20 seconds. Gene expression was normalized to PPIA using the 2-ΔΔCt method, and results are presented as fold change relative to E4. The primer sets used were listed in Table 1.

Quantification of HDL and VLDL Levels in E19 Chicken Embryo Plasma

The levels of HDL and VLDL in E19 chicken embryo plasma were determined using the Chicken High Density Lipoprotein ELISA Kit and Chicken Very Low Density Lipoproteins ELISA Kit (MyBioSource, San Diego, USA). A 500 μL of chicken embryo blood was centrifuged at 3,000 g for 10 minutes at 4°C. The supernatant was collected, mixed with the reaction reagent according to the kit protocol, and processed for absorbance measurement. Absorbance was measured at 450 nm using a spectrophotometer, and lipoprotein concentrations were quantified based on a standard curve.

Table 1
The primer of real-time quantitative PCR.

Gene	Primer sequence (5′- 3′)	Accession no.
PPIA (Internal control)	F: AGGTGCCCATAACAGCAGAG R: CACCACCCTGACACATGAAG	NM_00116632
APOA1	F:CCCGGCCCGGAGTTAATG R:AGGCCAAGCAACTTCGATCA	NM_205525.5
LCAT	F:AACTGGATGTGCTACCGCAA R:GTTCGGTTGTACACGACCCT	NM_001293094.2
ABCA1	F:AGCTGACCAAGGACCTGGAG R:CGTCCACTTGGCAGAGAACTG	XM_046905175.1
SOAT1	F:GAAGGGGCCTATCTGGAACG R:ATCTGCACGTGACATGACCA	NM_001039287.2
MTTP	F:TTCTGAAGGACATGCGTGCT R:GTCTAGGCCGTACGTGGATG	NM_0001109784.2
SAR1B	F: CATGTCCCCACACTACACCC R: TTTCCACACTCTGCGAGCTT	NM_001030621.2

Statistical analysis

Data were analyzed using Graph Pad Prism 9.0 (GraphPad Software Inc., La Jolla, CA, USA) and are presented as means ± SEM. For qPCR, statistical significance between two groups (E4 vs. E8) was assessed using an unpaired Student's t-test. For gene expression changes across embryonic development, a one-way analysis of variance (ANOVA) followed by Tukey's multiple comparisons test was applied. For HDL and VLDL levels in plasma, statistical significance between two groups was evaluated using an unpaired Student's t-test. p values ≤ 0.05 were considered statistically significant.

Results

Cell type identification in YSM by scRNA-seq

Single-cell RNA sequencing was performed on 9,037 cells from E4 and 6,884 cells from E7 YSM. UMAP analysis showed a clear separation between cells from the two stages (Fig. 1). Seventeen clusters were identified, and 11 major cell types were assigned based on the top 20 expressed in cluster and cross-referenced with specific markers reported in avian and mammalian literature (Supplementary Table 6-11): mesenchymal cells (Cluster 0), endodermal epithelial cells (Clusters 1, 2, 5), endodermal cells (Cluster 3), fibroblasts (Clusters 4, 13), vascular endothelial cells (Cluster 6), splanchnic mesoderm (Cluster 7), neurons (Clusters 8, 10, 16), hematopoietic stem cells (Cluster 9), epithelial cells (Clusters 11, 14), myocytes (Cluster 12), and myeloid cells (Cluster 15) (Fig. 1).

The relative composition of these cell types differed markedly between stages (Fig. 2). At E4, mesenchymal cells were the most abundant population (26.9%), followed by fibroblasts (15.2%). By E7, endodermal epithelial cells became dominant, with Clusters 1, 2, and 5 together accounting for 23.6%, 23.9%, and 19.3% of the total cells, respectively. Detailed cell numbers and percentages for all 17 clusters at E4 and E7 are summarized in Supplementary Table 5.

Functional characterization of EECs

Clusters 1, 2, and 5 were identified as EECs, with Cluster 2 showing the highest expression of epithelial markers such as E-cadherin (CDH1) and epithelial cell adhesion molecule (EpCAM), endodermal markers (Transthyretin/TTR, Alpha-Fetoprotein/AFP), and lipid metabolism genes (apolipoprotein A1/APOA1 and apolipoprotein C3/APOC3) (Table 2).

GO and KEGG enrichment of 113 upregulated genes at E7 showed enrichment in cholesterol metabolism, complement and coagulation cascades, fat digestion and absorption, and vitamin digestion and absorption pathways. The top GO terms were lipoprotein particle receptor binding, cholesterol transfer activity, and sterol transfer activity. Approximately 40% of genes in the apolipoprotein receptor binding pathway, including APOA1 and a homolog of an APOA2, were upregulated at E7 (Supplementary Table 6; Fig. 3).

Expression of HDL-related genes in EECs and temporal gene expression profiles in whole YSM

In EECs, APOA1 ranked 3rd in expression, whereas APOB ranked 63rd (Supplementary Table 6). APOA1, ATP Binding Cassette Transporter A1 (ABCA1), and lecithin cholesterol acyltransferase (LCAT) were significantly upregulated in EECs at E7 ($p < 0.05$) (Fig. 4A–C). To examine temporal expression dynamics across the full course of embryonic development, qPCR analysis was performed on whole YSM tissue collected at E4, E8, E12, E16, E20, and D3. Expression of HDL-associated genes (ABCA1, LCAT, APOA1, and SOAT1) increased progressively during incubation and peaked around E20 (Fig. 5A–C, G). In contrast, VLDL-related genes (APOB, MTTP, and SAR1B) exhibited

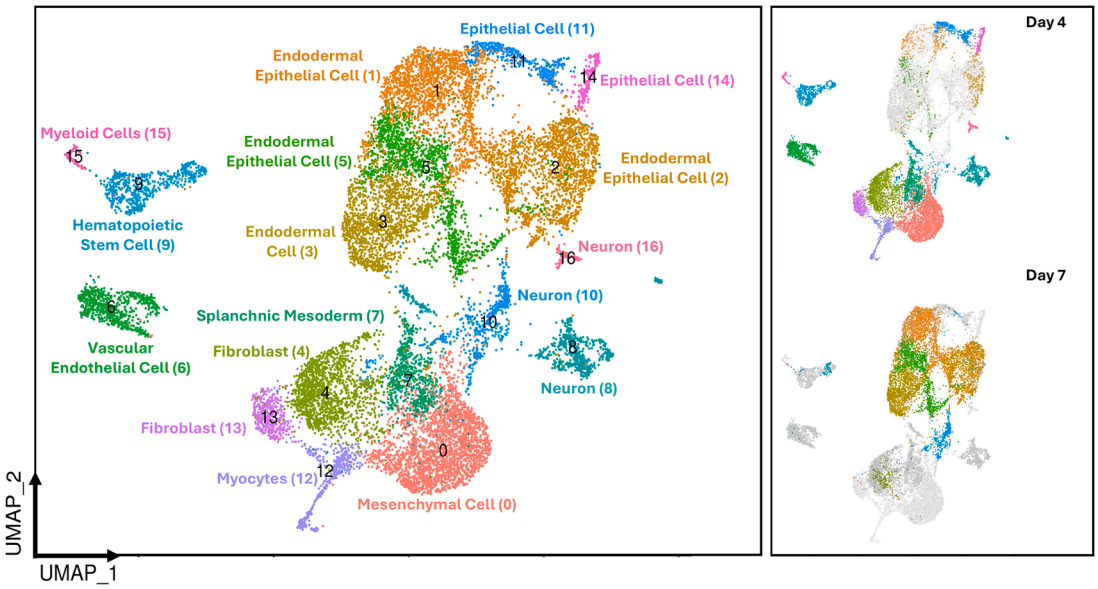

Fig. 1. scRNA-Seq analysis of embryonic chicken YSM at E4 and E7. UMAP projection of 15,921 single-cell transcriptomes clustered by gene expression and colored by cell type (cell cluster) (left). UMAP projection colored by cell type and split by developmental stage (E4 and E7, right). A total of 9,037 cells were analyzed at E4 and 6,884 cells at E7.

sustained upregulation throughout incubation, continuing to rise until hatching (Fig. 5D–F). Cholesteryl Ester Transfer Protein (CETP) was not detected in any cluster (Supplementary Fig. 3).

Plasma lipoprotein profiles reveal higher HDL than VLDL mass concentration at E19

To assess the relative importance of VLDL and HDL during late embryonic development, plasma lipoprotein levels were quantified at E19. HDL concentration (194.78 ± 30.13 mg/mL) was significantly greater than VLDL concentration (65.43 ± 13.82 mg/mL; $p < 0.01$) (Fig. 6), representing approximately 75% of total measured lipoproteins. Although this mass difference does not directly indicate transport dominance for specific lipid classes, as VLDL and HDL carry fundamentally different cargoes (triacylglycerols vs. cholesteryl esters and phospholipids, respectively), these data demonstrate that HDL is the more abundant lipoprotein by total mass in late-stage chicken embryo plasma.

Discussion

The present study provides a comprehensive transcriptomic characterization of the yolk sac membrane (YSM) during early chicken embryonic development, with particular emphasis on endodermal epithelial cells (EECs) and their role in lipoprotein metabolism. Using single-cell RNA sequencing, 17 transcriptionally distinct clusters in E4 and E7 YSM, among which EECs (Clusters 1, 2, and 5) demonstrated unique molecular features. Notably, APOA1 consistently ranked as the top apolipoprotein in clusters 2, whereas APOB ranked only 63rd, indicating a prominent role for the HDL-biogenesis program. These findings indicate that EECs, particularly Cluster 2, serve as the primary sites of HDL assembly and yolk lipid redistribution to the embryo.

Among the three endodermal epithelial clusters, Cluster 1 exhibited high expression of typical epithelial markers (EPCAM, CDH1, Keratin 7/KRT7, and β-keratins) (Patel and McGinnis, 1977; Yang et al., 2008; Wu et al., 2015; An et al., 2021) together with lipid metabolism and cholesterol homeostasis genes (Perilipin 2/PLIN2, Aldo-keto reductase 1D1/AKR1D1, Phospholipase A2 Group IIA /PLA2G2A, Cytochrome B5 Type A C/YB5A) (Hayashi et al., 2021; Zhang et al., 2022; Ma et al., 2024) (Supplementary Table 8). These features indicate that Cluster 1 represents an endodermal epithelial subtype with prominent barrier integrity and specialized lipid-transport capacity. Cluster 2, which showed the highest expression of both epithelial markers (CDH1, EPCAM) and HDL biosynthesis genes (APOA1, ABCA1, LCAT), appears to serve as the primary site of HDL assembly.

By contrast, Cluster 5 was characterized by high expression of lipid/cholesterol metabolism genes (PLA2G2A, Cell Death Inducing DFFA Like Effector A/CIDEA, and Intracellular cholesterol transporter/NPC2) and the endodermal transcription factor Forkhead box protein A1 (FOXA1) (Xu et al., 2019), but showed absent levels of classical epithelial markers (EPCAM and CDH1) (Supplementary Table 11). The co-expression of epithelial splicing regulatory protein 2 (ESRP2) and GATA binding protein 4 (GATA4) confirmed its endodermal identity (Geraud et al., 2017), whereas the dominant metabolic signature and immature epithelial phenotype suggest that Cluster 5 represents a metabolically specialized subtype. These three clusters likely reflect functional heterogeneity within the EEC population rather than a linear maturation hierarchy. Beyond delineating EEC heterogeneity, the dataset revealed that EEC clusters (Clusters 1, 2, and 5) are predominantly composed of E7 cells, with minimal representation at E4, indicating that a transcriptionally distinct EEC population with active lipoprotein biosynthesis programs has emerged by E7. Rather than representing temporal maturation within the same cell population, these findings suggest that E7 marks a developmental stage at which EECs have been specified and have acquired their characteristic transcriptional identity.

Previous studies have proposed the role of the yolk sac as the principal organ for lipid mobilization during late embryogenesis. Yadgary et al. (2013) reported about 50% decline in yolk lipid content between E11 and E21, underscoring the necessity of efficient lipid transport during this critical developmental stage. Earlier work by Hermann et al. (2000) and Bauer et al. (2013) suggested that EECs predominantly synthesize very-low-density lipoproteins (VLDL) for export into the embryonic circulation. However, our scRNA-seq data reveal a markedly different picture: KEGG pathway analysis showed significant upregulation of “Cholesterol metabolism” and “Fat digestion and absorption” pathways from E4 to E7. Consistently, APOA1 and HDL-related genes dominate EEC transcriptomes and increase progressively during incubation. At E19, plasma analysis confirmed that HDL mass concentration (194.78 ± 30.13 mg/mL) was significantly higher than that of VLDL (65.43 ± 13.82 mg/mL, $P < 0.01$).

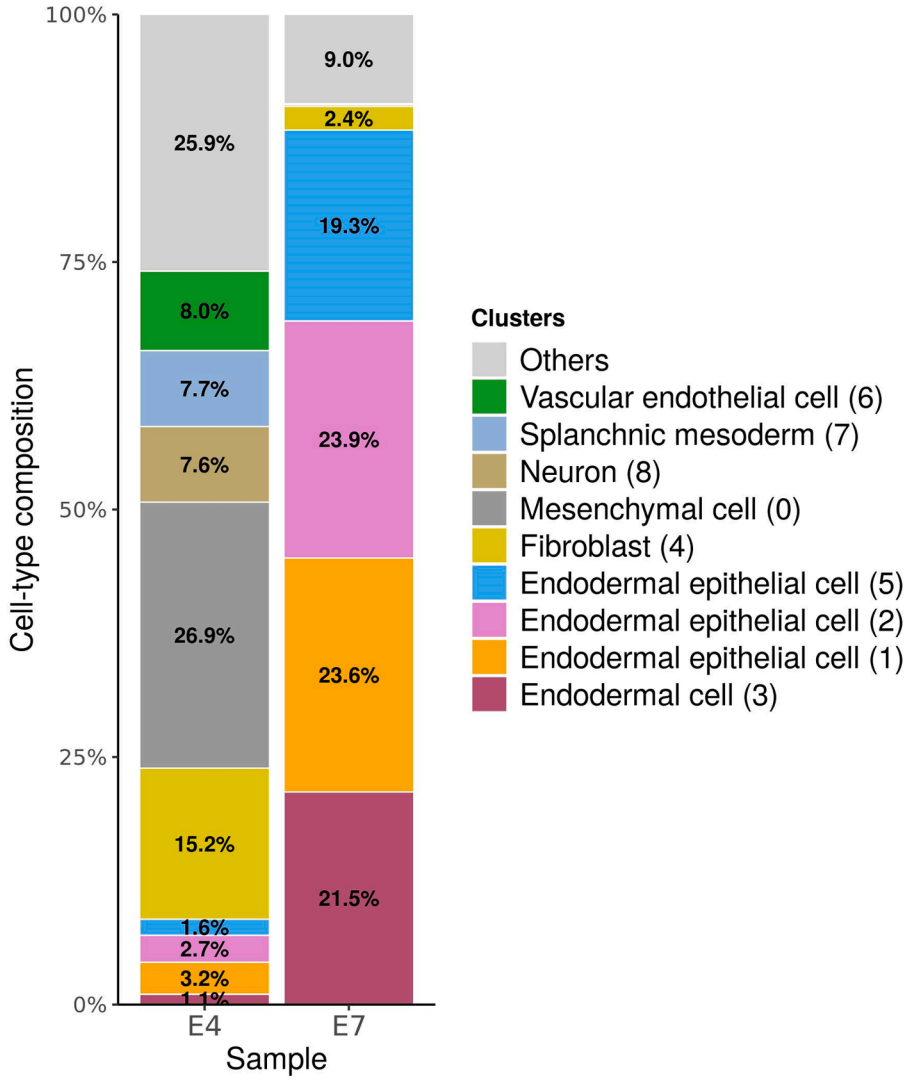

Fig. 2. Cell-type composition of the chicken yolk sac membrane at embryonic day 4 (E4) and day 7 (E7). Stacked bar plot showing the relative proportion of major cell types in E4 and E7 samples. Endodermal epithelial cells are divided into three distinct clusters (Clusters 1, 2, and 5). The numbers in the bars indicate the percentage of each cell type. Detailed cell numbers and percentages for all 17 clusters are provided in Supplementary Table 5.

Importantly, VLDL and HDL have distinct lipid transport functions. VLDL primarily carries triacylglycerols (~70% of its mass in avian species), whereas HDL is enriched in cholesteryl esters (CE, ~20%) and phospholipids (PL, ~30%) (Hermier et al., 1985). Using published compositional data for avian lipoproteins, we estimated that VLDL would transport approximately 45.8 mg/mL TAG but only 3.5 mg/mL CE, while HDL would carry approximately 39.0 mg/mL CE and 58.4 mg/mL PL but only 15.6 mg/mL TAG. Thus, VLDL remains the major TAG transporter, whereas HDL serves as the predominant carrier of cholesterol (free cholesterol + CE: ~48.7 mg/mL vs. ~5.5 mg/mL in VLDL) and phospholipids. These findings suggest a complementary rather than interchangeable role between VLDL and HDL during late embryogenesis.

The marked elevation of HDL during late incubation likely reflects the embryo's high demand for cholesterol to support rapid membrane biogenesis, organogenesis, and signaling pathways. Cholesterol is an essential structural component of cell membranes and a precursor for steroid hormones (Ikonen, 2008). However, excess free cholesterol is cytotoxic, as it can disrupt membrane fluidity, induce endoplasmic reticulum stress, and trigger apoptosis (Tabas, 2002; Song et al., 2021). To safely accommodate this demand, cholesterol is esterified into cholesteryl esters by SOAT1. The strong upregulation of SOAT1 observed in the yolk sac membrane during late incubation (Fig. 5G) (Ding and Lilburn, 2000; Wang et al., 2017) supports efficient conversion of free cholesterol into a less toxic storage and transport form. Together with the coordinated increase in HDL assembly genes, this mechanism may enable the embryo to mobilize cholesterol from residual yolk while minimizing lipotoxicity, representing a species-specific metabolic adaptation for late-stage development.

By E19, yolk TAG has been largely mobilized for energy production, while residual yolk is relatively enriched in cholesterol and CE. The progressive upregulation of HDL-associated genes (APOA1, ABCA1, LCAT, SOAT1) may therefore reflect a metabolic shift in the YSM toward cholesterol redistribution and phospholipid supply for rapid membrane biogenesis. This observation is consistent with previous reports by Kanai et al. (1996), who found HDL accounting for 54% of plasma lipoproteins at E15, and Hermier et al. (1985), who reported HDL as the predominant lipoprotein in five-week-old male broilers. It should be noted that our measurements represent a single late-stage time point and do not capture lipoprotein turnover rates. We therefore refrain from concluding overall "dominance" based solely on static mass concentrations.

Although VLDL has traditionally been regarded as the primary lipoprotein in embryonic avian plasma, our data highlight a previously underappreciated role for HDL during later stages of development.

Table 2
Top 20 highly expressed genes in endodermal epithelial cell cluster 2.

No.	Gene	Function	Note
1	TTR	Endodermal marker gene	
2	IFI6	Regulates apoptosis	
3	APOA1	Synthesizes high-density lipoprotein (HDL)	
4	AFP	Endodermal marker gene	
5	KRT40	Keratin family, cytoskeletal component of epithelial cells	
6	CDH17	Intestinal epithelial cells	
7	ALDOB	Involved in glycolysis, highly expressed in the liver	(Bu et al., 2018)
8	ENSGALG00015022000	Uncharacterized (Similar to Gallus gallus APOA2, 82% identity)	
9	TF	Transports iron to storage and utilization sites	
10	CDH1	Epithelial cell marker gene	(Ohgami et al., 2014)
11	B2M	Immune response	
12	EPCAM	Epithelial cell marker gene	(Gires et al., 2020)
13	FBP1	Involved in gluconeogenesis, highly expressed in the liver and kidneys	(Park et al., 2020)
14	TFF3	Secreted by intestinal goblet cells	(Yang et al., 2022)
15	AvBD10	Antimicrobial, aids in resistance to potential infections	(Mowbray et al., 2018)
16	RBP4A	Transports retinol from liver storage sites to peripheral tissues	
17	TSPAN8	Surface glycoprotein, interacts with integrins and participates in various biological functions	
18	FGG	Fibrinogen, a major component of blood clots	
19	SPP1	Cytokine, regulates IL-12 and IFN-γ	
20	APOC3	Component of VLDL, promotes VLDL assembly and secretion	

Concurrently, APOB, Microsomal triglyceride transfer protein (MTTP), and Secretion-associated and Ras-related (SAR1B) display a gradual but consistent upregulation in late-stage EECs (Fig. 5D-F), indicating that VLDL is also important in embryonic growth. Several non-mutually exclusive mechanisms may account for the late-stage upregulation of HDL-associated genes. First, as triacylglycerols in the yolk are progressively consumed for energy during mid-to-late incubation, the relative concentration of cholesterol and cholesteryl esters in residual yolk increases, which may serve as a metabolic signal for upregulation of HDL biosynthesis and cholesterol esterification pathways. Second, the cellular composition of the YSM likely changes during development, with EECs potentially undergoing further differentiation at later stages. The concurrent increase in SOAT1 and SAR1B expression at E20 may reflect a coordinated shift in EEC metabolic priorities from TAG processing toward cholesteryl ester packaging and lipoprotein secretion. Third, as the embryonic gut matures during late incubation, the YSM may progressively shift from a primary digestive and absorptive role toward specialized functions in cholesterol redistribution and reverse cholesterol transport. Thus, rather than replacing the established importance of VLDL, our findings demonstrate that HDL plays a substantially greater role than previously recognized during embryonic life, revealing a more complex and dynamic balance between HDL- and VLDL-mediated lipid transport than traditionally appreciated.

Collectively, these results indicate that, at least during late embryogenesis, the chicken embryo utilizes both HDL-mediated cholesteryl ester and phospholipid transport and VLDL-mediated triacylglycerol transport for energy supply and lipid redistribution, while simultaneously maintaining and strengthening VLDL-biogenesis machinery of undisputed importance in post-hatching avian metabolism. This revised perspective highlights the need to re-evaluate the relative contributions of HDL and VLDL across the full course of avian embryonic development.

Several limitations should be noted. First, plasma lipoprotein composition was assessed only at E19, precluding establishment of a full temporal profile across development. Second, we analyzed only two early time points (E4 and E7) by scRNA-seq; inclusion of late-stage samples (E15-E19) would provide direct transcriptomic evidence for

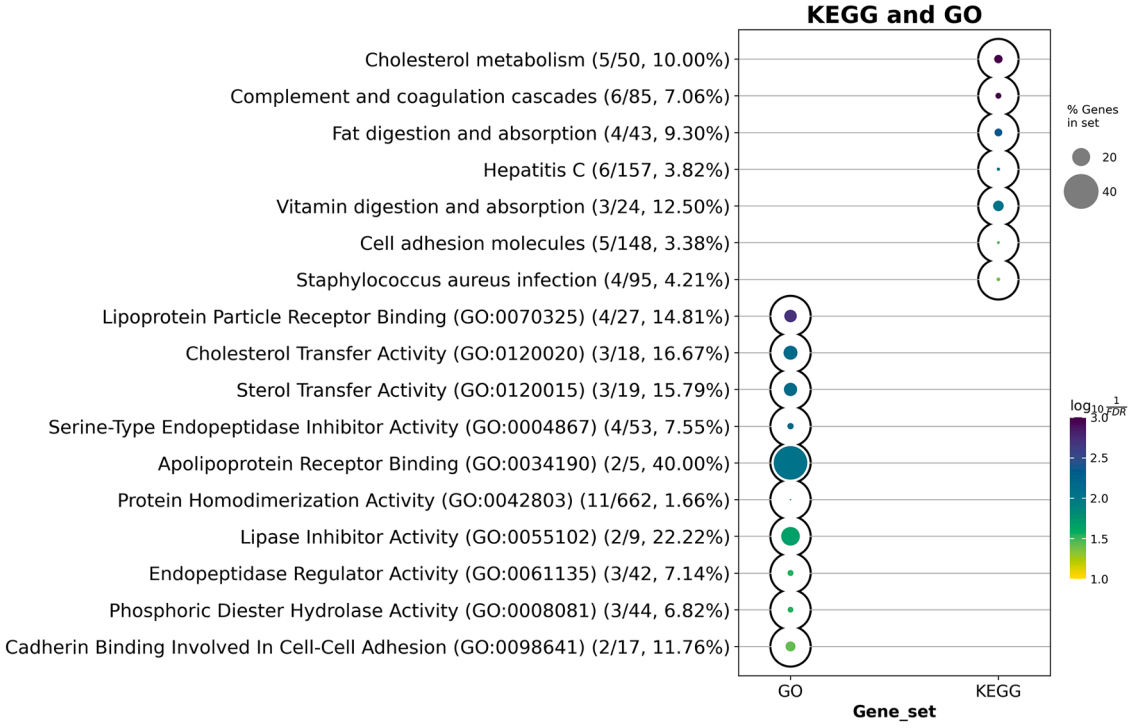

Fig. 3. Analysis of significantly enriched GO terms and KEGG pathways in Cluster 2, based on 113 upregulated genes between E4 and E7.

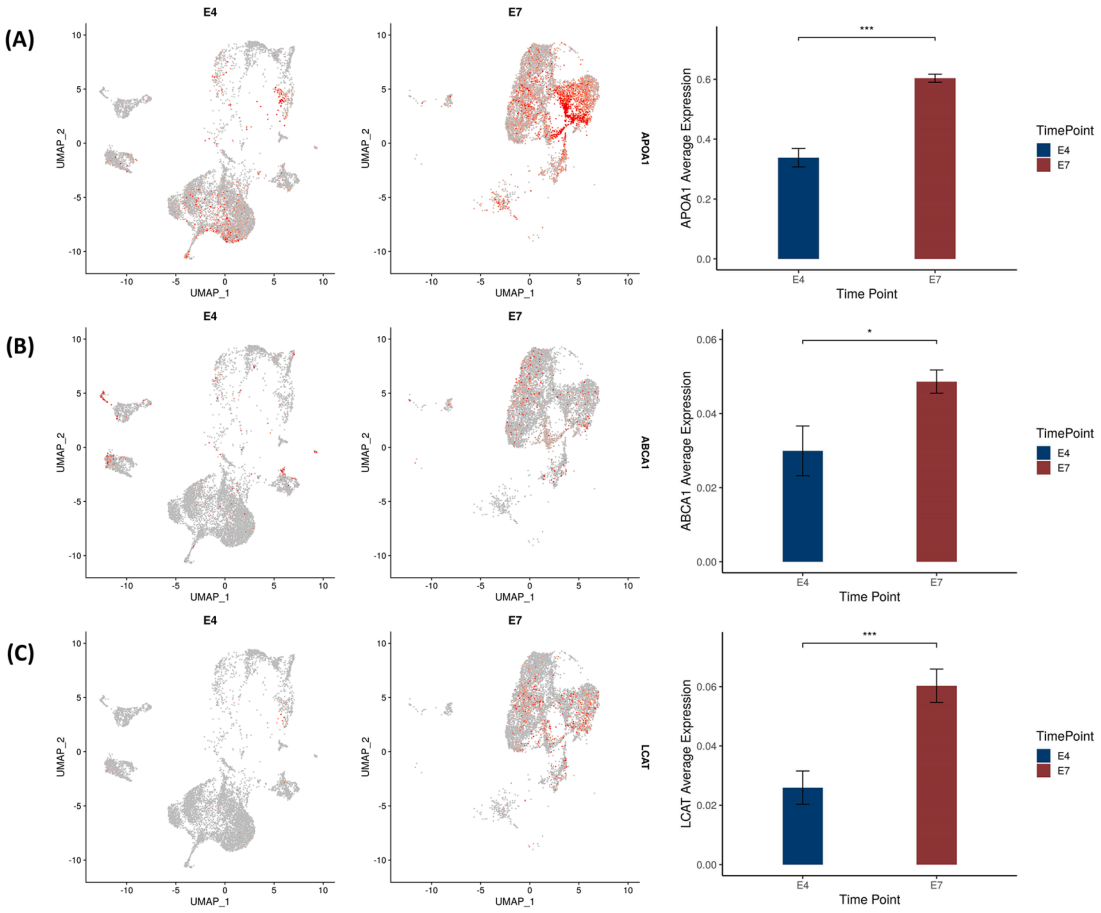

Fig. 4. Changes in HDL-related gene expression across YSM cell clusters and the average gene expression in EECs related cells (cluster 1, 2, 5). (A) APOA1; (B) ABCA1; (C) LCAT. Gene expression was calculated using log-normalized UMI counts. Darker colors indicate higher expression levels. Statistical significance between time points was determined using an unpaired t-test, with significance levels indicated (*p < 0.05, **p < 0.01, ***p < 0.001).

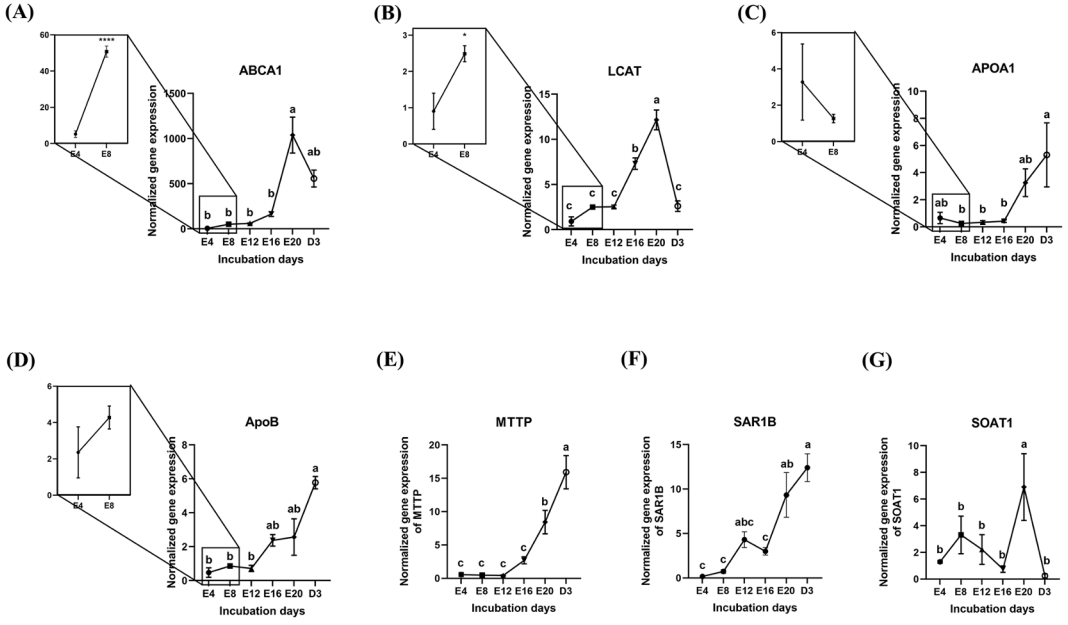

Fig. 5. The gene expression of HDL-related and VLDL-related genes in the YSM along embryo development. Data are presented as mean ± SEM. For gene expression changes across embryonic development, statistical results were analyzed by one-way ANOVA, and Tukey's multiple comparisons test; for gene expression change between E4 and E8, statistical results were analyzed by unpaired t-test (n = 5-10).

the HDL-to-VLDL transition. Third, direct functional validation of lipoprotein secretion by isolated EECs, such as pulse-chase labeling

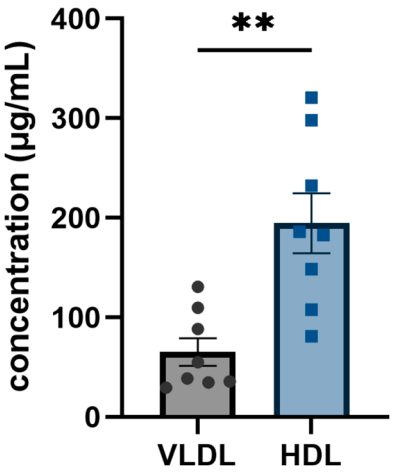

Fig. 6. Lipoprotein concentrations in plasma from E19 chicken. Statistical significance between two group was determined using an unpaired t-test, with significance levels indicated (**$p < 0.01$) ($n = 8$).

experiments or lipoprotein secretion assays, remains to be performed. Fourth, protein-level confirmation of APOA1 and APOB by immunohistochemistry or Western blotting would strengthen our mRNA-based conclusions. Finally, the functional consequences of the higher HDL mass concentration for embryonic growth and hatchability warrant investigation. Despite these limitations, our work provides the first single-cell evidence that HDL plays a more substantial role than previously recognized in mediating cholesteryl ester and phospholipid transport during avian embryonic development, complementing the established importance of VLDL in triacylglycerol transport and laying the foundation for future studies on avian-specific metabolic adaptations.

Funding

Funds supporting this study were provided by the National Science and Technology Council, R.O.C. (project no. 113-2313-B-002 −008 -MY3; project no. 114-2313-B-002 −043 -MY3)

Data availability

The scRNA-seq data generated in this study have been deposited in the NCBI BioProject database under accession number PRJNA1451834. The data can be accessed at: https://www.ncbi.nlm.nih.gov/bioproject/?term=PRJNA1451834. All other data supporting the findings of this study are available within the article and its supplementary materials.

CRediT authorship contribution statement

Jie-Ci Wu: Writing – review & editing, Writing – original draft, Validation, Methodology, Formal analysis, Data curation, Conceptualization. **Zhao-Qi Hu:** Formal analysis, Data curation. **Yuan-Yu Lin:** Writing – review & editing, Writing – original draft, Supervision, Methodology, Data curation, Conceptualization. **Harry J. Mersmann:** Writing – review & editing, Writing – original draft. **Shih-Torng Ding:** Writing – review & editing, Writing – original draft, Supervision, Methodology, Funding acquisition, Conceptualization.

Disclosures

The authors declare that they have no conflict of interest.

Acknowledgements

We thank the Animal Resource Center and the Consortium of Integrative Biomedical Science Key Technology at National Taiwan University for their technical support.

Supplementary materials

Supplementary material associated with this article can be found, in the online version, at doi:10.1016/j.psj.2026.106950.

References

Amer, M.F., 1962. Embryonic mortality and malpositions in Fayoumi Chicken. Poult. Sci. 41 (6), 1707. https://doi.org/10.3382/ps.0411707. −+.

An, Q., Liu, T., Wang, M.Y., Yang, Y.J., Zhang, Z.D., Liu, Z.J., Yang, B., 2021. KRT7 promotes epithelial-mesenchymal transition in ovarian cancer via the TGF-beta/Smad2/3 signaling pathway. Oncol. Rep. 45 (2), 481–492. https://doi.org/10.3892/or.2020.7886.

Bauer, R., Plieschnig, J.A., Finkes, T., Riegler, B., Hermann, M., Schneider, W.J., 2013. The developing chicken yolk sac acquires nutrient transport competence by an orchestrated differentiation process of its endodermal epithelial cells. J. Biol. Chem. 288 (2), 1088–1098. https://doi.org/10.1074/jbc.M112.393090.

Ding, S.T., Lilburn, M.S., 2000. The developmental expression of acyl-coenzyme A: cholesterol acyltransferase in the yolk sac membrane, liver, and intestine of developing embryos and posthatch turkeys. Poult. Sci. 79 (10), 1460–1464. https://doi.org/10.1093/ps/79.10.1460.

Ding, S.T., Lilburn, M.S., 2002. The ontogeny of fatty acid-binding protein in turkey (Meleagridis gallopavo) intestine and yolk sac membrane during embryonic and early posthatch development. Poult. Sci. 81 (7), 1065–1070. https://doi.org/10.1093/ps/81.7.1065.

Eresheim, C., Plieschnig, J., Ivessa, N.E., Schneider, W.J., Hermann, M., 2014. Expression of microsomal triglyceride transfer protein in lipoprotein-synthesizing tissues of the developing chicken embryo. Biochimie 101 (100), 67–74. https://doi.org/10.1016/j.biochi.2013.12.020.

Geraud, C., Koch, P.S., Zierow, J., Klapproth, K., Busch, K., Olsavszky, V., Leibing, T., Demory, A., Ulbrich, F., Diett, M., Singh, S., Sticht, C., Breitkopf-Heinlein, K., Richter, K., Karppinen, S.M., Pihlajaniemi, T., Arnold, B., Rodewald, H.R., Augustin, H.G., Schledzewski, K., Goerdt, S., 2017. GATA4-dependent organ-specific endothelial differentiation controls liver development and embryonic hematopoiesis. J. Clin. Invest. 127 (3), 1099–1114. https://doi.org/10.1172/JCI90086.

Gires, O., Pan, M., Schinke, H., Canis, M., 2020. Expression and function of epithelial cell adhesion molecule EpCAM: where are we after 40 years? Cancer Metastasis Rev. 39 (3), 969–987. https://doi.org/10.1007/s10555-020-09898-3.

Bu, P., Chen, K.Y, Xiang, K., Johnson, C., Crown, S.B., Rakhilin, N., Ai, Y., Wang, L., Xi, R., Astapova, I., Han, Y., Li, J., Barth, B.B., Lu, M., Gao, Z., Mines, R., Zhang, L., Herman, M., Hsu, D., Zhang, G.F., and Shen, X.. 2018. Aldolase B-Mediated fructose metabolism drives metabolic reprogramming of colon cancer liver metastasis. Cell Metab 27(6):1249–1262 e1244. https://doi.org/10.1016/j.cmet.2018.04.003.

Hayashi, D., Mouchlis, V.D., Dennis, E.A., 2021. Omega-3 versus Omega-6 fatty acid availability is controlled by hydrophobic site geometries of phospholipase A2s. J. Lipid Res. 62. https://doi.org/10.1016/j.jlr.2021.100113, 100113.

Hermann, M., Mahon, M.G., Lindstedt, K.A., Nimpf, J., Schneider, W.J., 2000. Lipoprotein receptors in extraembryonic tissues of the chicken. J. Biol. Chem. 275 (22), 16837–16844. https://doi.org/10.1074/jbc.M000163200.

Hermier, D., Forgez, P., Chapman, M.J., 1985. A density gradient study of the lipoprotein and apolipoprotein distribution in the chicken, Gallus domesticus. Biochim. Biophys. Acta 836 (1), 105–118. https://doi.org/10.1016/0005-2760(85)90226-7.

Ikonen, E., 2008. Cellular cholesterol trafficking and compartmentalization. Nat. Rev. Mol. Cell Biol. 9 (2), 125–138. https://doi.org/10.1038/nrm2336.

Kanai, M., Soji, T., Sugawara, E., Watari, N., Oguchi, H., Matsubara, M., Herbert, D.C., 1996. Participation of endodermal epithelial cells on the synthesis of plasma LDL and HDL in the chick yolk sac. Microsc. Res. Tech. 35 (4), 340–348. https://doi.org/10.1002/(SICI)1097-0029(19961101)35:4<340::AID-JEMT5>3.0.CO;2-Q.

Ma, M.Y., Deng, G., Zhu, W.Z., Sun, M., Jiang, L.Y., Li, W.H., Liu, Y.B., Guo, L., Song, B. L., Zhao, X.L., 2024. Defects in CYB5A and CYB5B impact sterol-C4 oxidation in cholesterol biosynthesis and demonstrate regulatory roles of dimethyl sterols. Cell Rep. 43. https://doi.org/10.1016/j.celrep.2024.114912, 114912.

Mowbray, C.A., Niranji, S.S., Cadwell, K., Bailey, R., Watson, K.A., 2018. Gene expression of AvBD6-10 in broiler chickens is independent of AvBD6, 9, and 10 peptide potency. Vet. Immun. Immunopathol 202, 31–40. https://doi.org/10.1016/j.vetimm.2018.06.007.

Ohgami, R.S., Chisholm, K.M., Ma, L., 2014. E-cadherin is a specific marker for erythroid differentiation and has utility, in combination with CD117 and CD34, for enumerating myeloblasts in hematopoietic neoplasms. Am. J. Clin. Pathol. 141 (5), 656–664. https://doi.org/10.1309/AJCP8M4QQTAZPGRP.

Park, H.J., Jang, H.R., Park, S.Y., Kim, Y.B., Lee, H.Y., 2020. The essential role of fructose-1,6-bisphosphatase 2 enzyme in thermal homeostasis upon cold stress. Exp. Mol. Med. 52 (3), 485–496. https://doi.org/10.1038/s12276-020-0402-4.

Patel, M.B., McGinnis, J., 1977. Effects of protein and fat in the diets on hatchability of eggs and chick growth. Poult. Sci. 56 (2), 529–537. https://doi.org/10.3382/ps.0560529.

Peñuela, S., Hernandez, V., 2018. Characterization of embryonic mortality in broilers. Rev Mvz Cordoba 23 (1), 6500–6513. https://doi.org/10.21897/rmvz.1245.

Shand, J.H., West, D..W., McCartney, R.J., Noble, R.C., Speake, B.K., 1993. The esterification of cholesterol in the yolk sac membrane of the chick embryo. Lipids 28 (7), 621–625. https://doi.org/10.1007/BF02536056.

Song, Y., Liu, J., Zhao, K., Gao, L., Zhao, J., 2021. Cholesterol-induced toxicity: an integrated view of the role of cholesterol in multiple diseases. Cell Metab. 33 (10), 1911–1925. https://doi.org/10.1016/j.cmet.2021.09.001.

Tabas, I., 2002. Consequences of cellular cholesterol accumulation: basic concepts and physiological implications. J. Clin. Invest. 110 (7), 905–911. https://doi.org/10.1172/JCI16452.

Tung, C.T., Lin, H..J., Lin, C.W., Mersmann, H.J., Ding, S.T., 2021. The role of dynamin in absorbing lipids into endodermal epithelial cells of yolk sac membranes during embryonic development in Japanese quail. Poult. Sci. 100 (11), 101470. https://doi.org/10.1016/j.psj.2021.101470.

Wang, S.H., Lin, H..J., Lin, Y.Y., Chen, Y.J., Pan, Y.H., Tung, C.T., Mersmann, H.J., Ding, S.T., 2017. Embryonic cholesterol esterification is regulated by a cyclic AMP-dependent pathway in yolk sac membrane-derived endodermal epithelial cells. PLoS One 12 (11), e0187560. https://doi.org/10.1371/journal.pone.0187560.

Wu, P., Ng, C.S., Yan, J., Lai, Y.C., Chen, C.K., Lai, Y.T., Wu, S.M., Chen, J.J., Luo, W., Widelitz, R.B., Li, W.H., Chuong, C.M., 2015. Topographical mapping of alpha- and beta-keratins on developing chicken skin integuments: functional interaction and evolutionary perspectives. Proc. Natl. Acad. Sci. U S. A 112 (49), E6770–E6779. https://doi.org/10.1073/pnas.1520566112.

Xu, Y., Zhang, Q., Tan, L., Xie, X., Zhao, Y., 2019. The characteristics and biological significance of NPC2: mutation and disease. Mutat. Res. Rev. Mutat. Res. 782, 108284. https://doi.org/10.1016/j.mrrev.2019.108284.

Yadgary, L., Kedar, O., Adepeju, O., Uni, Z., 2013. Changes in yolk sac membrane absorptive area and fat digestion during chick embryonic development. Poult. Sci. 92 (6), 1634–1640. https://doi.org/10.3382/ps.2012-02886.

Yadgary, L., Wong, E.A., 2014. Temporal transcriptome analysis of the chicken embryo yolk sac. BMC Genom. 15 (1), 690. https://doi.org/10.1186/1471-2164-15-690.

Yang, Y., Lin, Z., Lin, Q., Bei, W., 2022. Pathological and therapeutic roles of bioactive peptide trefoil factor 3 in diverse diseases: recent progress and perspective. Cell Death Dis. 13 (1), 62. https://doi.org/10.1038/s41419-022-04504-6.

Yang, W., Qiu, C., Biswas, N., Jin, J., Watkins, S.C., Montelaro, R.C., Coyne, C.B., Wang, T., 2008. Correlation of the tight junction-like distribution of Claudin-1 to the cellular tropism of hepatitis C virus. J. Biol. Chem. 283 (13), 8643–8653. https://doi.org/10.1074/jbc.M709824200.

Zhang, M., Xiang, R., Glorieux, C., Huang, P., 2022. PLA2G2A Phospholipase promotes fatty acid synthesis and energy metabolism in pancreatic cancer cells with K-ras mutation. Int. J. Mol. Sci. 23, 11721. https://doi.org/10.3390/ijms231911721.